A

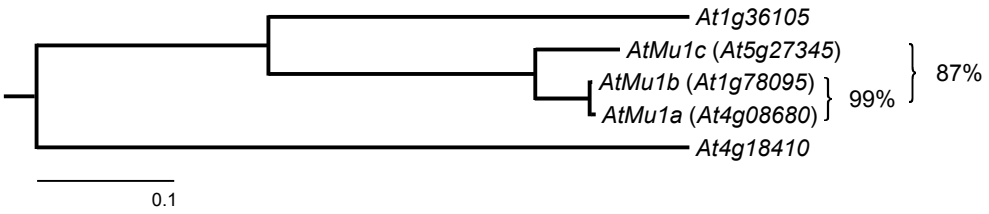

B

```
                                                  SNP1 (MspI)
AtMu1a    TAGTTGCTCACCTAATGGGAAATGTCAGATCTTGAAGAGTCCTGTAATTGCTAGGTTGTT 60
AtMu1b    TAGTTGCTCACCTAATGGGAAATGTCAGATCTTGAAGAGTCCTGTAATTGCTAGGTTGTT 60
AtMu1c    TAGTTGCTCACCTAATGGGAAATGTCAGATCTTAAAGAGTCCGGTAATTGCTAGGTTGTT 60
          ************************ ******* ******** ******************
                    SNP2 (DdeI)
AtMu1a    TTTGGACAAGCTGAGGCTAAATGAGAAGTTTATGCCTATGGATATTCAGGAATATATCAA 120
AtMu1b    TTTGGACAAGTTGAGGCTAAATGAAAAGTTTATGCCTATGGATATTCAGGAATATATCAA 120
AtMu1c    CTTGGACAAGCTGAGGATAGATGAAAAGTTTATGCCTATGGATATTCAGCTATATATCAA 120
           ********* ***** ** **** ************************  *********

AtMu1a    AGAGCGTTGGAAAATGGTGTCTACAATCCCACAATGCC                       158
AtMu1b    AGAGCGTTGGAAAATGGTGTCTACAATCCCACAATGCC                       158
AtMu1c    AGAGCGTTGGAAATTGGTGTCTACAATCCCACAATGCC                       158
          ************* ************************
```

AtMu1 copy	SNP1 (*Msp*I, CCGG)	SNP2 (*Dde*I, CTNAG)	Number of clones	
			Col	L*er*
AtMu1a	No	Yes	0	0
AtMu1b	No	No	0	0
AtMu1c	Yes	Yes	26	26

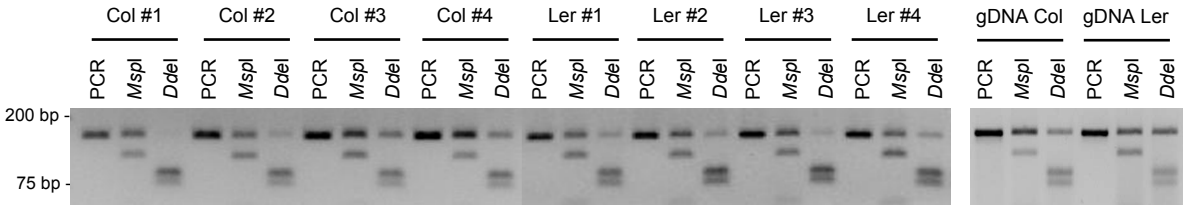

Supplemental Figure 1: *AtMu1* phylogeny in Col and transcript discrimination assay.

(A) Phylogenetic analysis of the five *AtMu1* copies from Col. The values indicate sequence identities of the whole transposon region (including TIRs) between different copies. The scale bar represents the genetic distance. *At1g36105* and *At4g18410* were not analyzed further in this study. (B) *AtMu1* transcript discrimination assay. A 158 bp fragment of *AtMu1* was digested with *Msp*I (SNP1) or *Dde*I (SNP2), respectively. SNP1 was specific for *AtMu1c*, SNP2 was specific for *AtMu1b*. Restriction enzyme recognition sites are highlighted in yellow, SNPs disrupting recognition sites are marked in red. 26/26 clones analyzed for each Col and L*er* originated from *AtMu1c*. Bottom panel: Example for the *AtMu1* transcript discrimination assay. Purified products of PCR reactions on individual subcloned fragments for four Col and four L*er* clones were digested with *Msp*I or *Dde*I. Digestion by *Msp*I and *Dde*I indicates the clone originated from *AtMu1c*.

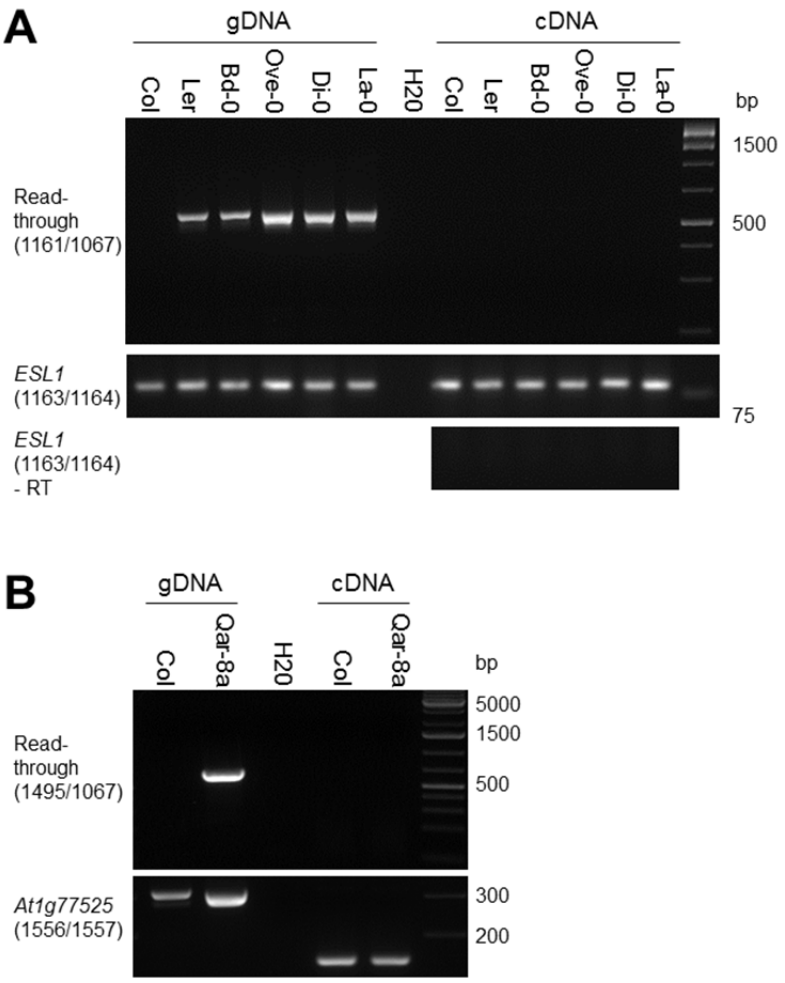

Supplemental Figure 2: Absence of read-through transcription from the adjacent gene into *AtMu1c* inserted into annotat ed 3' UTRs (Chr. 1: 2.9 Mb; Chr. 1: 29.1 Mb).

PCR was performed on genomic DNA (gDNA) and cDNA of the indicated accessions using a forward primer in (A) *ESL1* (L*er* group, Chr. 1: 2.9 Mb, Primer 1161) or (B) *At1g77525* (Qar-8a, Chr. 1: 29.1 Mb, Primer 1495) and a reverse primer in the TIR of *AtMu1c* (Primer 1067). *ESL1* and *At1g77525* transcript levels were monitored as controls using the indicated primer pairs.

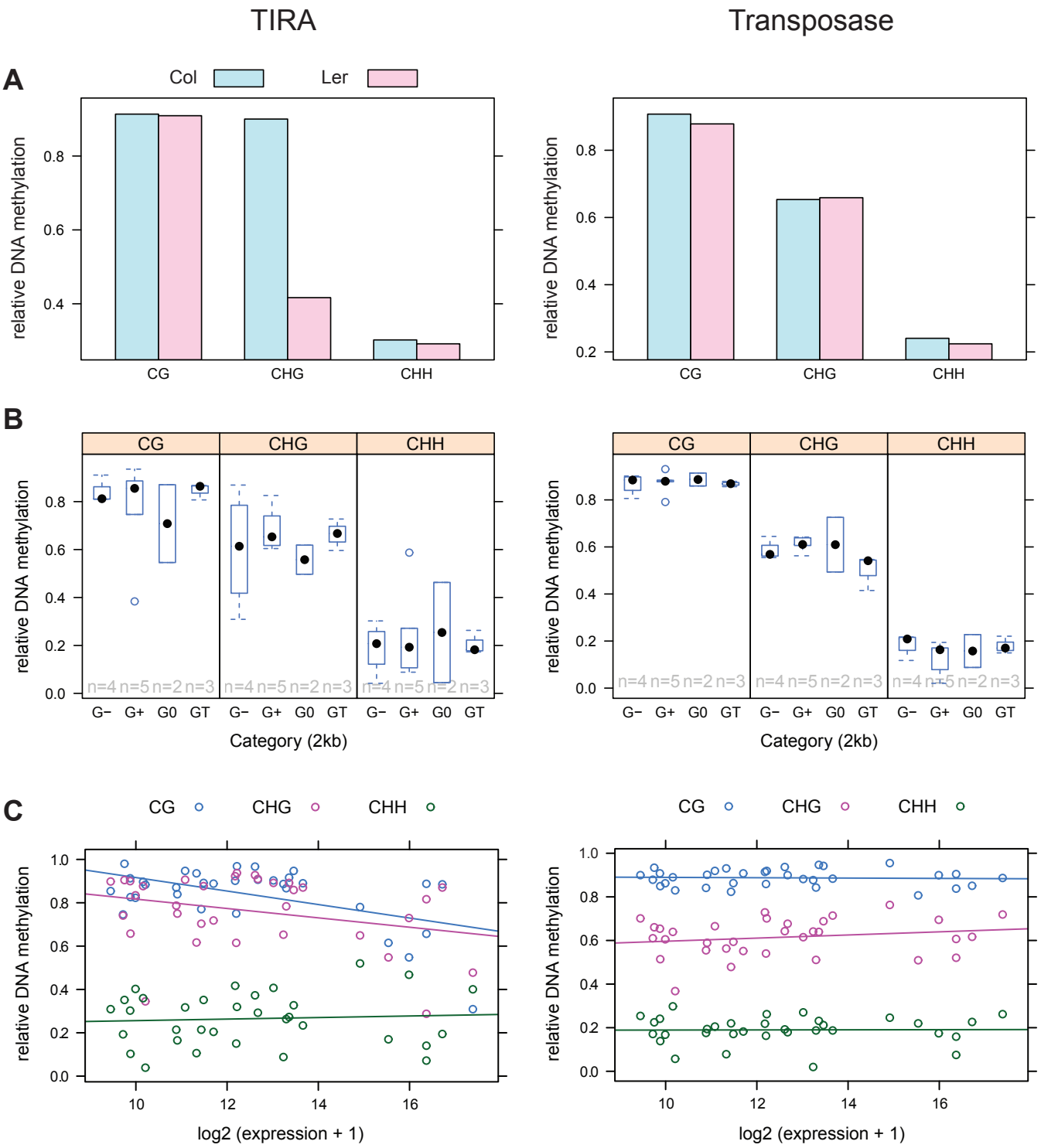

Supplemental Figure 3: Global DNA methylation analysis of *AtMu1c* based on BS-seq methylome data.

(A) Processed BS-seq reads from Col and L*er* were reanalyzed for reads mapping to *AtMu1c* TIRA or transposase. (B) *AtMu1c* DNA methylation for different categories of insertion sites and different sequence contexts (CG, CHG, CHH). Methylation data from accessions with only one *AtMu1c* insertion were used. Methylation values for accessions with the same insertion site were averaged to avoid weighing of insertion frequencies. Differences in the number of analyzed insertion sites are caused by the lack of methylome data for some accessions. See Figure 6B for corresponding expression analysis. (C) Scatterplot with regression lines of DNA methylation in different sequence contexts and *AtMu1c* expression (based on RNA-seq data) for accessions with a single *AtMu1c* copy and detectable *AtMu1c* expression.

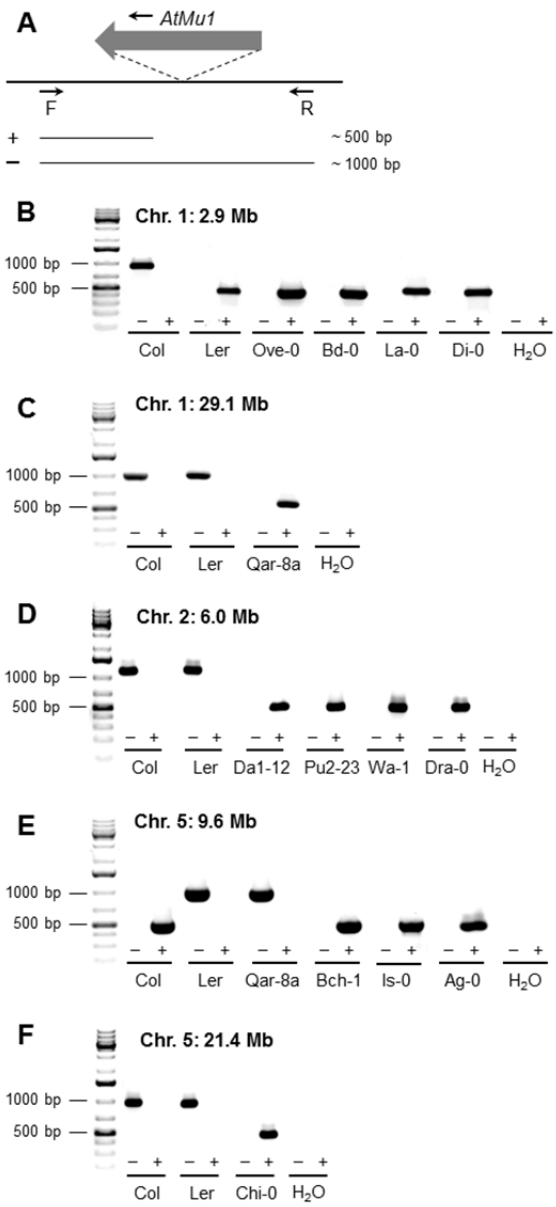

Supplemental Figure 4: Experimental validation of novel *AtMu1c* insertion sites.

(A) Schematic representation of validation strategy. In the absence of the insertion in the indicated accession, flanking primers F and R will give a product of ca. 1000 bp (-) and no product will be produced with F and the *AtMu1c*-specific primer 1067 (+). Conversely, if the insertion is present in the indicated accession, there will be a product only in the (+) reaction (ca. 500 bp). (B-F) Experimental validation of the *AtMu1c* insertion at Chr. 1: 2.9 Mb (B); Chr. 1:29.1 Mb (C); Chr. 2: 6.0 Mb (D); Chr. 5: 9.6 Mb (E); Chr. 5: 21.4 Mb (F).

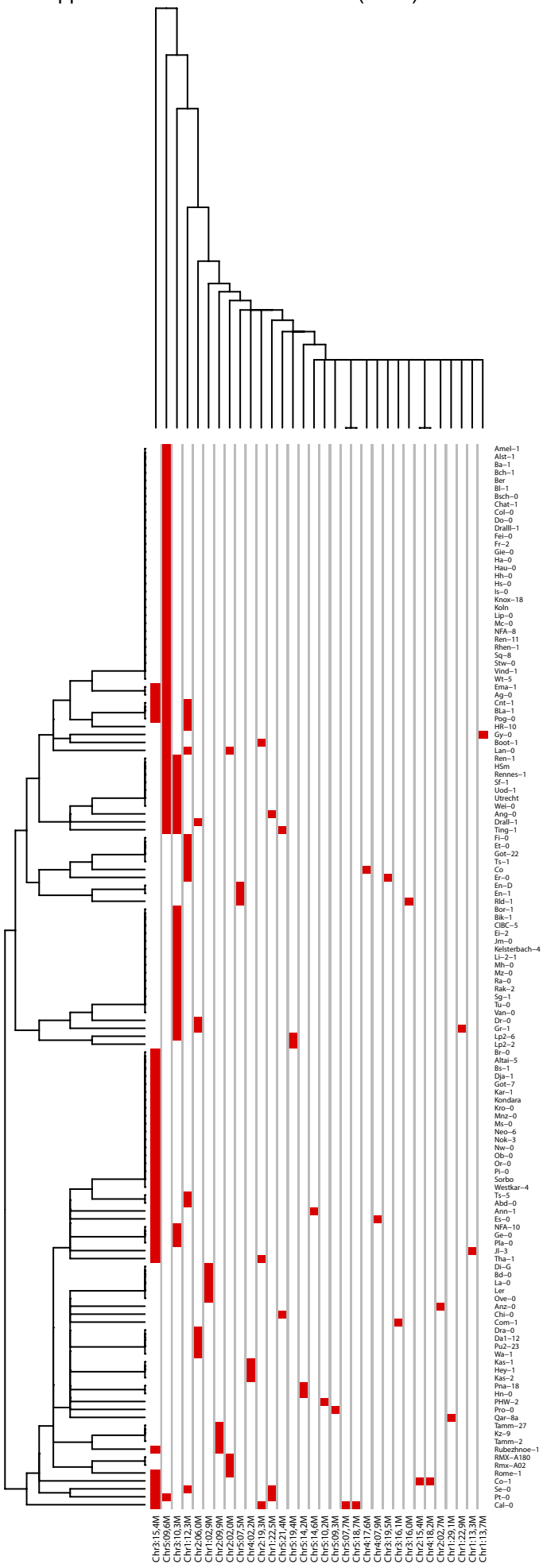

Supplemental Figure 5: Mosaic table of *AtMu1c* insertion sites in accessions. Binary heat map representing presence of insertion sites (red) across analyzed accessions with at least one copy of *AtMu1c*. Accessions were clustered according to their *AtMu1c* insertion sites.

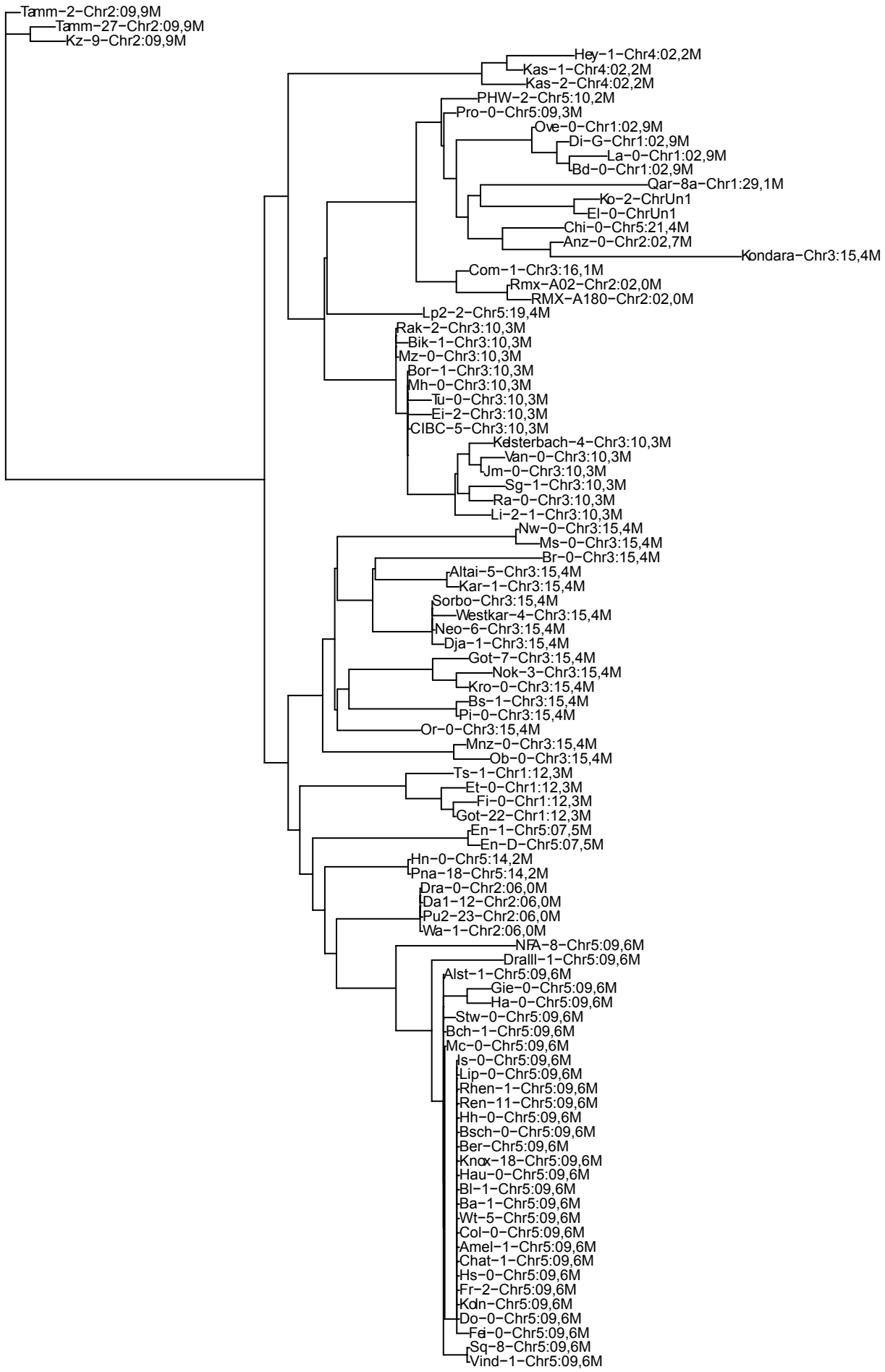

Supplemental Figure 6: Phylogenetic clustering of *AtMu1c* from accessions with single *AtMu1c* copies indicates clustering of accessions with insertion position. The phylogenetic tree is based on *AtMu1c* consensus sequences (including TIRs and transposase) from accessions with a single *AtMu1c* insertion. Accession names and insertion sites are indicated.

Supplemental Table 1: Comparison of *AtMu1* TIR sequences.

	TIR length (bp)	**Number of SNPs between Col TIRA und TIRB (percent identity)**	**Identity between TIRs of indicated *AtMu1* copies**
AtMu1a	TIRA: 296 TIRB: 296	7 (97.64%)	TIRA (1a/1c): 68% TIRB (1a/1c): 72%
AtMu1b	TIRA: 296 TIRB: 296	11 (96.28%)	TIRA (1b/1a): 96% TIRB (1b/1a): 97%
AtMu1c	TIRA: 295 TIRB: 286	17 (94.57%) and 9 bp deletion (91.19%) L*er*: 18 (93.90%) and 9 bp deletion (90.85%)	TIRA (1b/1c): 67% TIRB (1b/1c): 71%

Supplemental Table 2: Details of bisulfite sequencing *AtMu1c* (cf. Figure 4B). H is A, C or T; N is any nucleotide.

		CG	CHG	CHH	number of clones analyzed
number of sites in sequence analyzed		4	7	67	
number of sites analyzed	NIL9.9.15 (Col)	92	161	1541	23
	NIL9.9.3 (L*er*)	92	161	1541	23
proportion of methylated C	NIL9.9.15 (Col)	0.337	0.130	0.031	
	NIL9.9.3 (L*er*)	0.370	0.062	0.002	

Supplemental Table 3: List of primers used in this study.

Target	Primer	Sequence (5' → 3')	Experiment	Comment
ibid5	188/ibid5 F 189/ibid5 R	AATAAAGCAAGAAAGCAAGTCTT TCCATCAAATCTCATGTTGAAC	Mapping	
PERLx473	PERLx473_F PERLx473_R	AAGGTTGAGGTAACTGTGAAAGCAA CGTATTCCGAGAACTCCAGATCA	Mapping	
dCAPS2.88	407/DCAPS 2.88 F 408/DCPAS 2.88 R	GCGATACACCACAGTGAAGAAGAGATCTT GATGCAATGAACAAGAATCGTTTGA	Mapping	
ibid9	ibid9_F ibid9_R	GAGAAAATTACTTTACTTAAATTACGCA ACAGGTAATTGTGGATTATGAAGGA	Mapping	
PERLx779	203/PERLx779 F 204/PERLx779 R	TCCAAGAGTAATGGTAGACTAGAG GCTCTTTGATTGCATTTGAGG	Mapping	
ibid7	195/ibid7 F 196/ibid7 R	CATTTACATTACAACTACTGGTGT ACAGGCAGGGGTTGTACC	Mapping	
AtMu1 unspliced (a, b, c)	45/Mu1 134/Mu1 intron1 F	GCTCTTGCTTTGGTGATGGT GGTATGTAACGAAGTTCTCATTATG	RT-PCR	
AtMu1 spliced (a,b,c)	44/Mu1 45/Mu1	CCGAGAACTGGTTGTGGTTT GCTCTTGCTTTGGTGATGGT	RT-PCR	(Singer et al., 2001)
AtMu1a,b,c	496/Mu discri F 497/ Mu discri R	TAGTTGCTCACCTAATGGGAAATGT GGCATTGTGGGATTGTAGACAC	AtMu1 transcript discrimination assay	
AtMu1c	1006/PyroMark_F1 1007/PyroMark_R1 1008/PyroMark_S1	Biotin-GACAGCCACCATGCCATTAA GCGACTCATTCTTCCCTTTGATC GGTGCGGTTACCAAG	Pyrosequencing	
AtMu1c	1249/Bisulf_Mu5g_TIR_BottomStrand 1319/Bisulf_Mu5g_TIR_TopStrand_II	ATAAAAAAATCRAACCCTCCTTACCAAAC GGGTTGTTTGCTTYTGTTATTYTGAA	Bisulfite sequencing	
AtMu1c	720/Mu5g left F 721/Mu5g left R	GTGATCAAGACATCATGTACGCAT CATTGTGGGATTGTAGACACCAA	Methylation assay, ChIP	Fig. 3: left
AtMu1c	943/Mu5g middle F 944/Mu5g middle R	TCAAGAAGAATCATGCCAAGAA GCGGTTCCTCTTTCAATACATC	Methylation assay, ChIP	Fig. 3: middle
AtMu1c	722/Mu5g right F 723/Mu5g right R	GAAGAATGAGTCGCCAAAA TCTCTTTCTCGGGACCTTCTCC	Methylation assay, ChIP	Fig. 3: right
AtMu1c	1067/Mu5g TIR F 1068/Mu5g TIR R	TGGTTGGGTCAATGGTTTAATAGC CTGCCTCTGTCACCCTGAAATA	Methylation assay, ChIP	Fig. 3D: TIR, Fig. 3: Primer 5, 6
ESL1	1161/ESL1_F 1162/ESL1_R	GAAACTAAAGGAAGAACATTGGA CCCTATCACTATCCGTATCTGAAA	PCR	Fig. 3: Primer 1, 2
AtMu1c	1085/AtMu1.5g_F 1086/AtMu1.5g_R	CGGCTAAACCTGTAGTGT AATAACAGTGGATTTTAAGGTGA	PCR	Fig. 3: Primer 3, 4
TUB6	161/TUB6 RT F 160/TUB6 RT R	GGTGAAGGAATGGACGAGAT GTCATCTGCAGTTGCGTCTT	qPCR	
AtMu1a,b,c	459/Muq3 R 460/Muq3 F	TTTTACATCGTAATGCGTTATGCC GAAGAATGAGTCGCCAAAGAAGAA	qPCR	
ESL1	1163/ESL1-F-qRT 1164/ESL1-R-qRT	CGATGTCGGAGAACTCAAGA GCAGTGATACGACATTCGTTG	RT-PCR	(Yamada et al., 2010)
At1g77525	1556/Qar8a_qPCR_F 1557/Qar8a_qPCR_R	GAAATCTGTTAGTGCGTGTGTGG CACTGTTGAGGACCCCGAG	RT-PCR	

Chr. 1: 29.1 Mb	1494/Qar-8a_Mu_F 1495/Qar-8a_Mu_R	GATATTTTCCTGCGTGGGTT GTGTGTGGTTCTTTGTGTTCTC	PCR	
Chr. 2: 6.0 Mb	1496/MADS_Box_Intron_F 1497/MADS_Box_Intron_R	GTGTAGACTTCCGTGCAGGT ACGATTTTTCATTTTTGTAGCA	PCR	
Chr. 5: 21.4 Mb	1498/Chi-0_Mu_F 1499/Chi-0_Mu_R	GAGGAGTGGAGCATGGAAG ATGACAATTGCGTGGAAGTAG	PCR	

Supplemental References

Singer, T., Yordan, C., and Martienssen, R.A. (2001). Robertson's Mutator transposons in A. thaliana are regulated by the chromatin-remodeling gene Decrease in DNA Methylation (DDM1). Genes Dev **15,** 591-602.

Yamada, K., Osakabe, Y., Mizoi, J., Nakashima, K., Fujita, Y., Shinozaki, K., and Yamaguchi-Shinozaki, K. (2010). Functional analysis of an Arabidopsis thaliana abiotic stress-inducible facilitated diffusion transporter for monosaccharides. J Biol Chem **285,** 1138-1146.